Kinetic modeling of ultraintense x-ray laser-matter interaction

- study of saturable absorption of XFEL and IP depression -

Yasuhiko Sentoku

Institute of Laser Engineering
Osaka University

High Z Ion Acceleration

Laser

	Case I. Previous J-KAREN
pulse duration	36 fs (FWHM)
spot radius at 1/e^2	3.4 μm
laser pulse energy	8 J
peak irradiance	1×10^{21} W/cm^2
contrast ratio	10^{10}
incidence angle to target	45°, p-pol

Al 0.8um, Fe 10nm

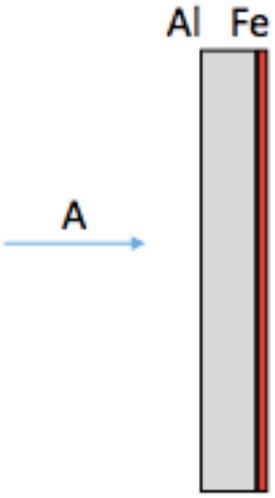

Pre-plasma 中のイオン価数	+3
Pre-plasma length (um)	~20
Sc(um)	~6

On the surface of the Fe layer, place H_2O(10nm) as contamination layer.

Electron energy density and iron energy density snapshot every 6.6 fs; total 50 frames

electron

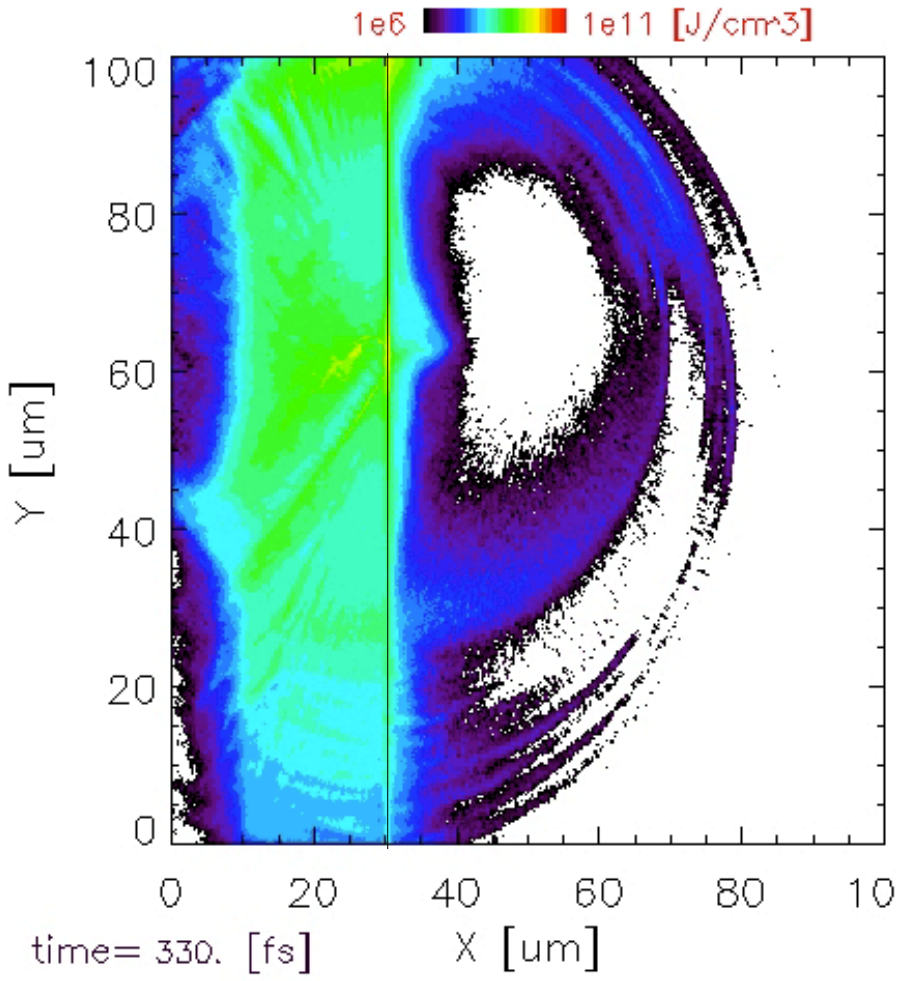

iron

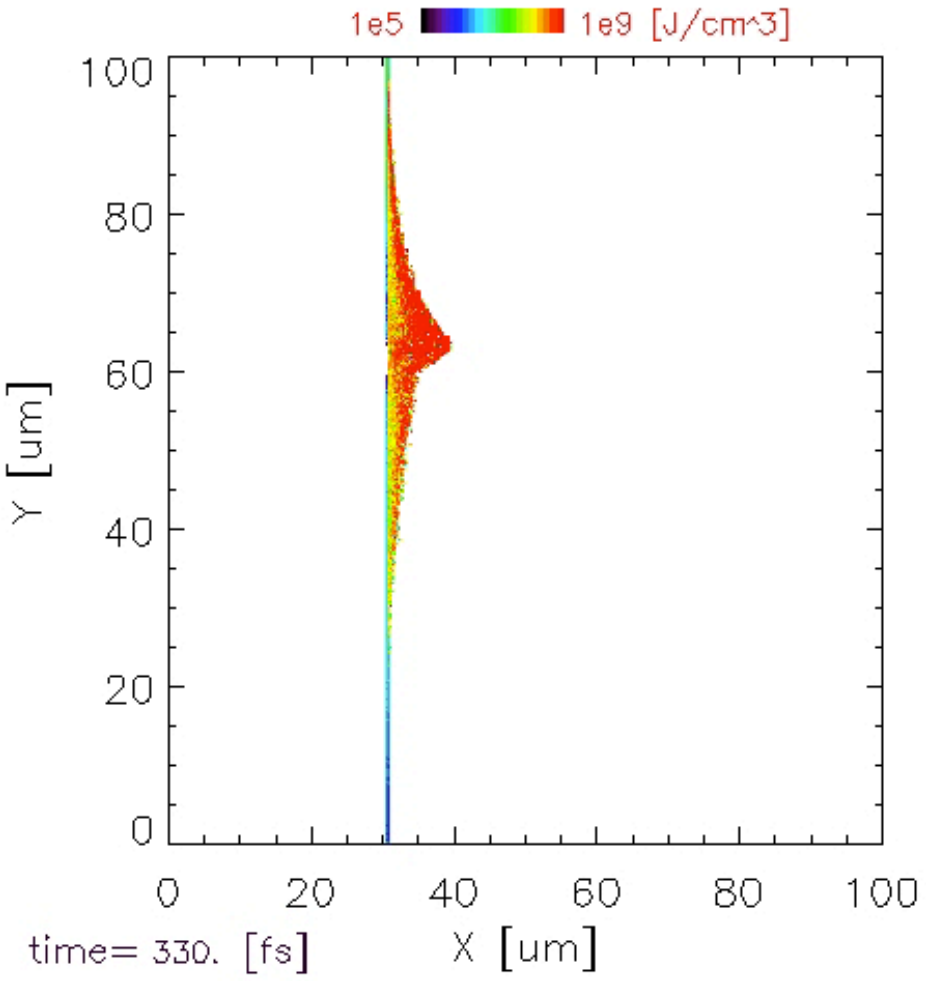

Time evolution of iron charge state

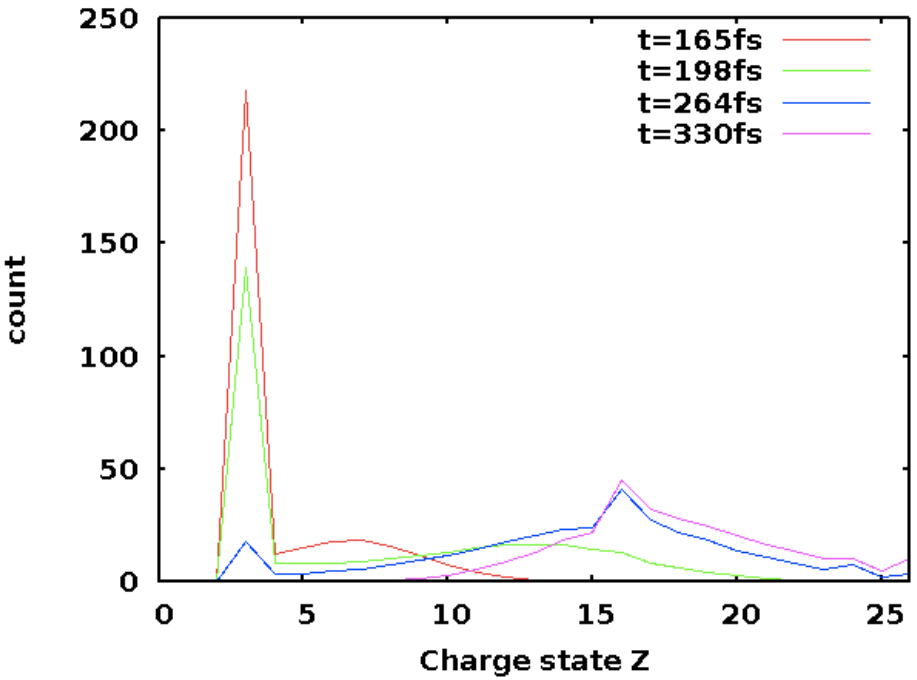

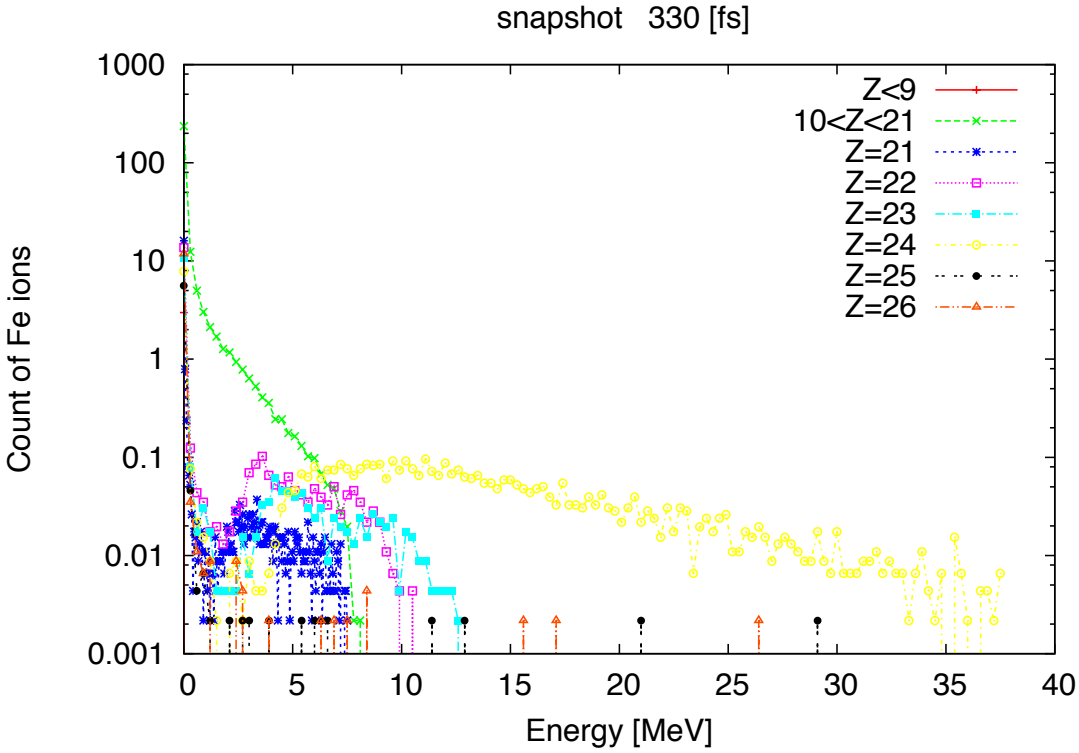

This has both impact ionization and field ionization.

Motivation

The ionization processes are important for the plasma formation simulation.

Is your ionization calculation correct?

The ionization models are ok?
field, impact, photo

Ionization potentials are accurate enough?
Ionization potential depression(IPD)
blueshift of orbital energy with charge state

In this talk, let’s see the IPD model.

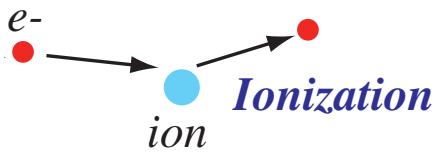

Model of Impact Ionization

Lotz formula

$$\sigma_{col} = \sum_{i=1}^{N} a_i q_i \frac{\ln(E/P_i)}{EP_i} \left\{1 - b_i \exp\left[-c_i(E/P_i - 1)\right]\right\}, \; E \geq P_i$$

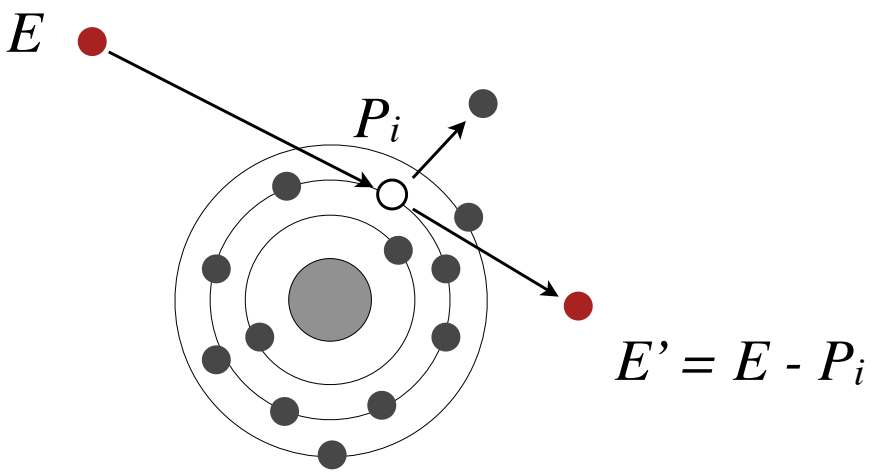

The probability of the impact ionization using Lotz formula.

$$P = \sigma_{col} n_h v_e \Delta t$$

When a uniform random number r [0,1)
r < P
an electron is born and the impact electron loses energy.

E: the energy of the impact electron.
P_i: the orbital energy of electron in the i-th shell.
q_i: the number of equivalent electrons in i-th shell.
a_i, b_i, and c_i: individual constants.

This is a model for a free standing atom

W. Lotz, Z. Physik **232**, 101 (1970)

Ionization potentials are reduced in dense plasmas: Ionization Potential Depression(IPD)

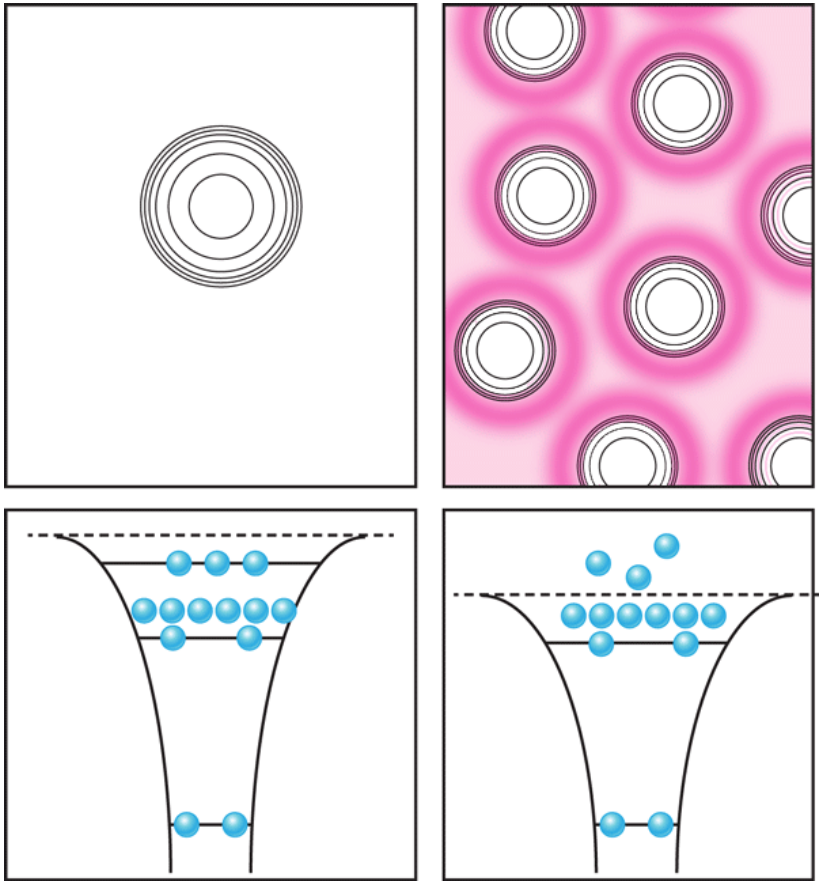

Electron and ion fields compete with atomic field and can effectively lower the ionization potential P_i, so that the ionization cross-section.

Ionization potential (IP) depression model in dense plasmas

Electron and ion fields compete with atomic field and can effectively lower the IP of an ion, affecting the charge state distribution.

J. Stewart and K. Pyatt, The Astrophysical Journal (1966)

$$\Delta E_{\mathrm{SP}} = 2.16 \times 10^{-7} \frac{Z_i + 1}{r_i} \left(\left(1 + \left(\frac{r_D}{r_i} \right)^3 \right)^{2/3} - \left(\frac{r_D}{r_i} \right)^2 \right) \quad (\mathrm{eV}),$$

$$r_D = 743.4 \left(\frac{T_e}{n_e (1 + \bar{Z})} \right)^{1/2}$$ Deybe radius

$$r_i = \left(\frac{3\bar{Z}}{4 n_e} \right)^{1/3}$$ ion sphere radius

G. Ecker and W. Kröll, Phys. of Fluids (1963)

$$\Delta E_{\mathrm{EK}} = (Z_i + 1)(\bar{Z} + 1)^{1/3} u_{\mathrm{WS}}$$

$$u_{\mathrm{WS}} = \frac{e^2}{4\pi\epsilon_0 R_{\mathrm{WS}}}$$ Wigner-Seitz energy

$$R_{\mathrm{WS}} = \left(\frac{3}{4\pi n_i} \right)^{1/3}$$ Wigner-Seitz radius

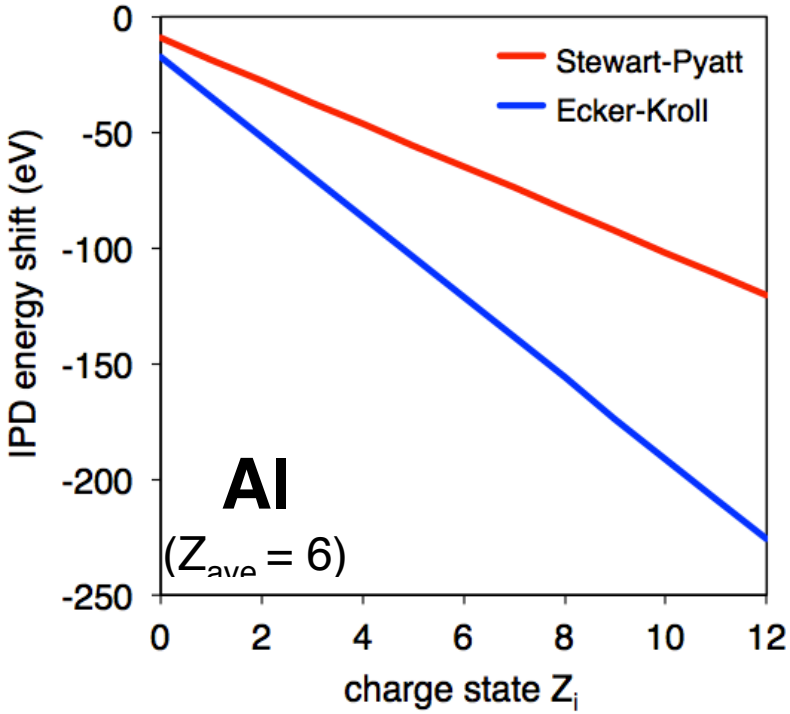

using XFEL check the IPD model

Limitations of atomic kinetics modeling

A custom version of **SCFLY** (Super-Configuration FLYCHK) is the modeling tool of choice for XFEL—matter interaction studies and has been quite successful, but has limitations.

Pros

- Rate equations include many atomic processes to self-consistently determine SC level populations.
- Can accurately calculate evolution of CSD, T_e, n_e, opacities and emitted spectra.

Cons

- Model is **zero-dimensional**: each simulation is provided a single intensity and calculates a single T_e, n_e, transmission, etc.
- Accounting for spatial variation is cumbersome and not self-consistent.
- **Does not account for plasma dynamics!**

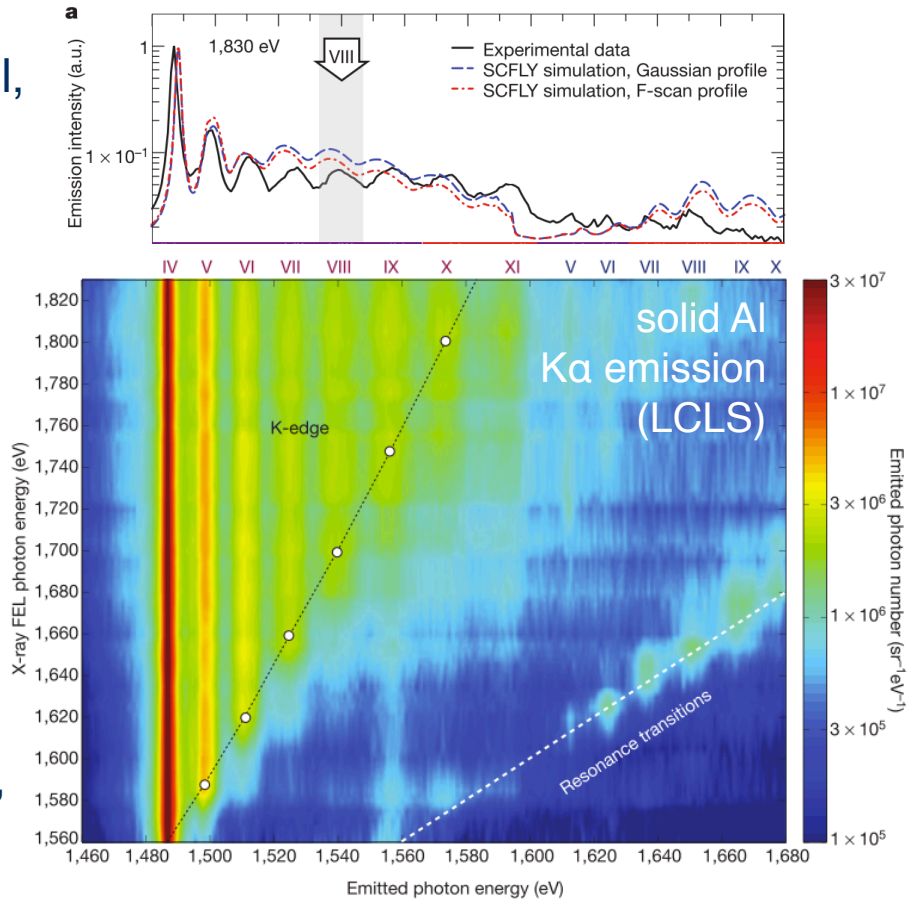

—S. M. Vinko *et al.*, Nature (2012)

PICLS + Radiation Transport:
radiation physics in kinetic plasmas

I. γ-ray emissions by intense laser light

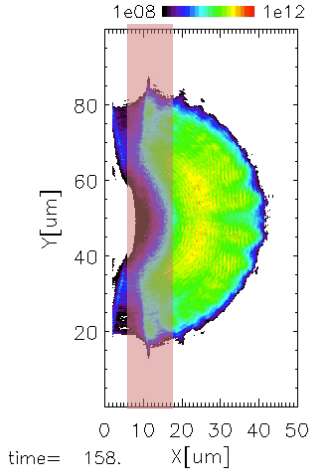

Hard x-rays emissions via bremsstrahlung and radiative damping in laser - plasma interaction are simulated in the radiation transport calculation.

bremsstrahlung from a thin copper foil

II. x-ray transport in laser-plasma interaction

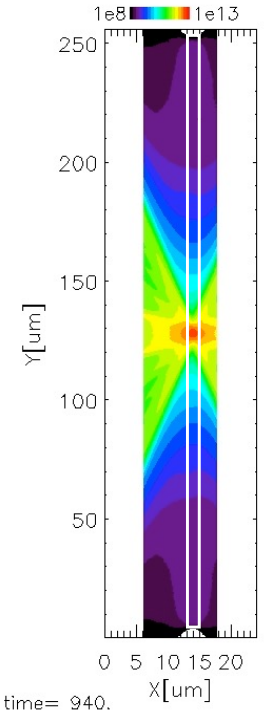

X-ray emissions and absorptions via bound-bound, bound-free, free-free, and characteristic emissions are simulated using NLTE opacity and emissivity database.

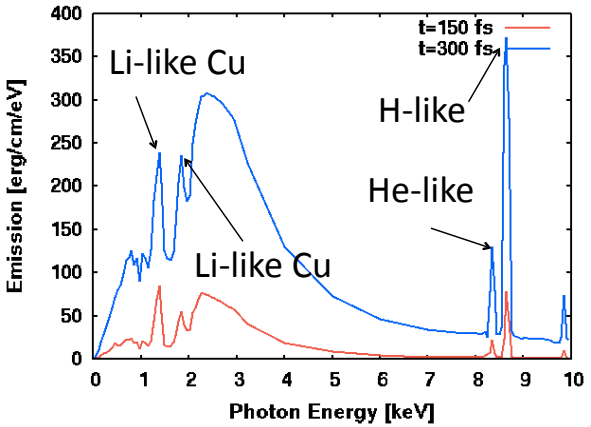

K-α emission

III. Intense x-rays and matter interaction

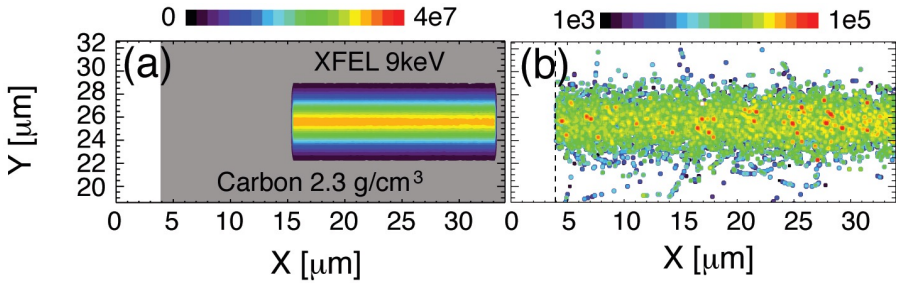

Photoionization for keV photons including both radiative and non-radiative (auger) processes is simulated for intense x-ray laser - matter interaction. Photoelectrons and auger electrons are thermalized via collisional processes.

XFEL and solid carbon interaction

Radiation transport model for intense laser-produced plasmas

Radiative transfer equation

$$\left(\frac{1}{c}\frac{\partial}{\partial t}+\mathbf{n}\cdot\nabla\right)I=\eta-\chi I$$

- $I(\mathbf{r},\Omega,h\nu,t)$: intensity of radiation
- $\eta(\mathbf{r},h\nu,t)$: emissivity
- $\chi(\mathbf{r},h\nu,t)$: opacity

(a) CIP (Constrained Interpolation Profile) scheme for advection

CIP scheme having 3rd order spatial accuracy is applied for advection term. Because of explicit method, this scheme is suitable for MPI.

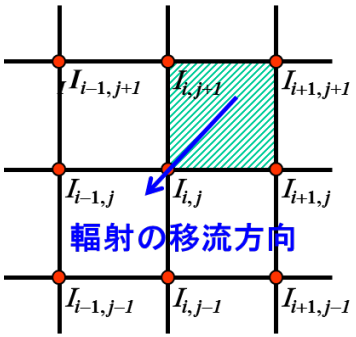

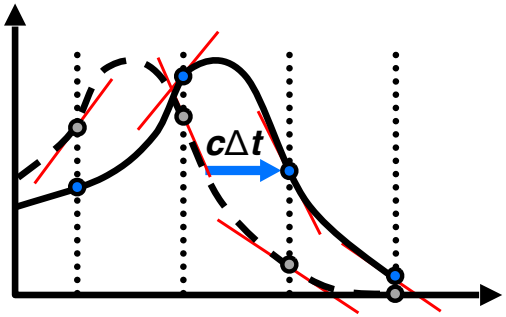

T. Yabe, et al., CPC **66** (1991) 233.; F. Xiao et al., CPC **93** (1996) 1; F. Xiao et al., CPC **94** (1996) 103.

(b) S_N method for direction

For the angular variables (polar angle θ and azimuthal angle ω), we apply the discrete ordinate method. The transport equation is solved for each discrete direction (m,n) to obtain the radiation intensity in that direction, $I_{m,n}$

Lee, C.E., Los Alamos Scientific Laboratory Report LA-2595, 1962

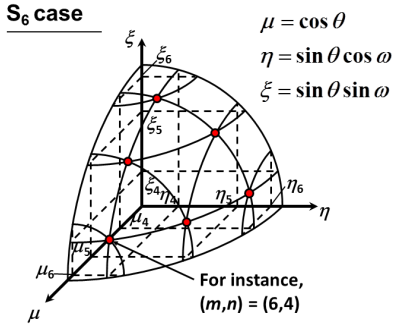

This method allows us to simulate anisotropic emission!

(c) Multi-group method for photon energies

Radiation energy is divided into groups of finite energy width. The transport equation is integrated over the energy width for each group, then solved to obtain the radiation intensity for each group, I_g.

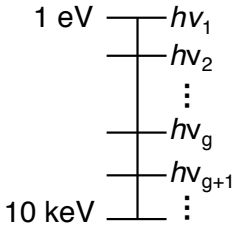

$$I_g(r,\Omega,t)=\int_{h\nu_{g+1}}^{h\nu_g} I(r,\Omega,h\nu,t)dh\nu$$

$$\eta_g(r,\Omega,t)=\int_{h\nu_{g+1}}^{h\nu_g} \eta(r,\Omega,h\nu,t)dh\nu$$

$$\tilde{\chi}_{a\,g}(r,t)=\int_{h\nu_{g+1}}^{h\nu_g} \tilde{\chi}_a(r,h\nu,t)dh\nu$$

Radiation transport in a PIC code

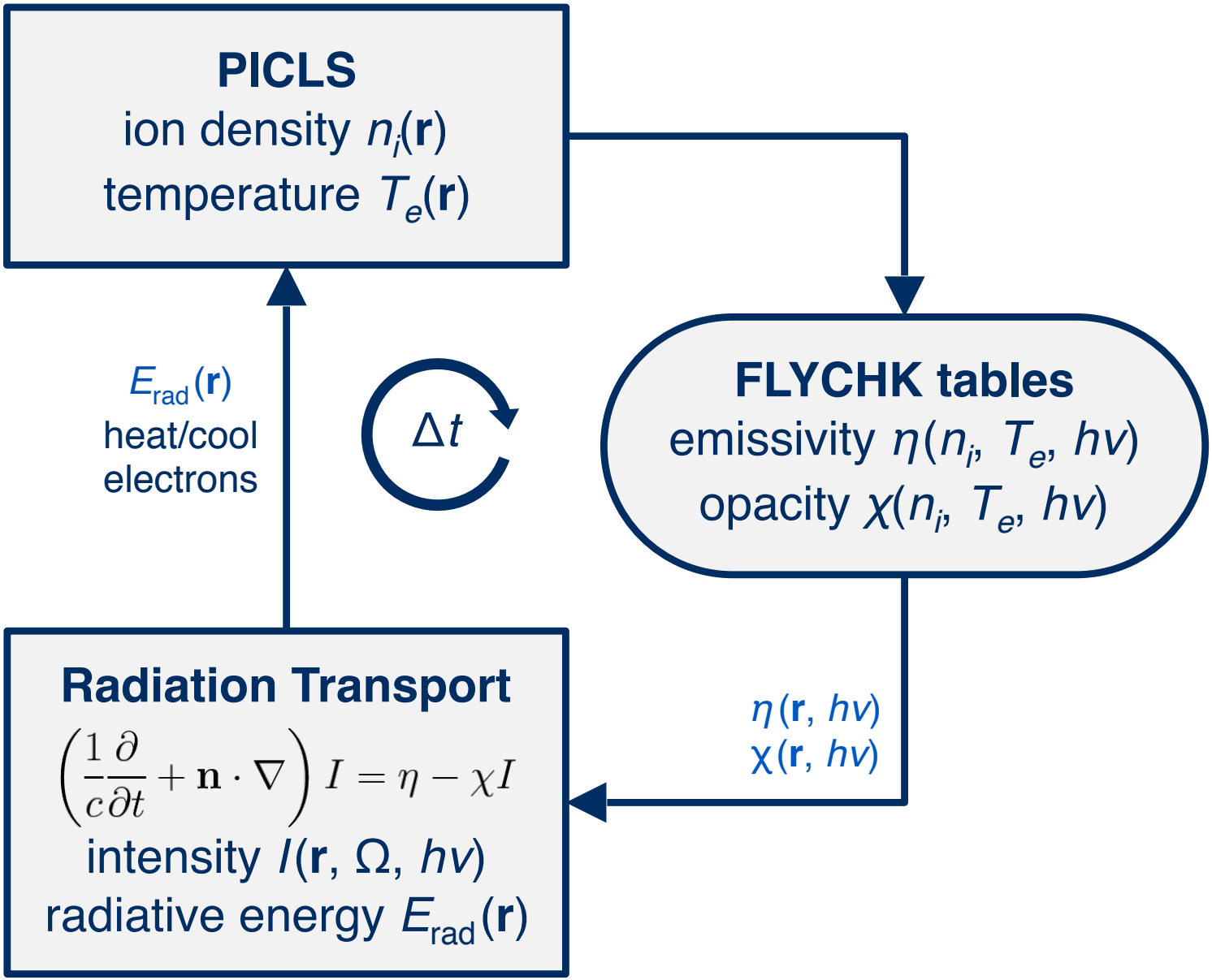

By solving radiation transport, we can get spatiotemporal x-ray information

Radiation transport code (RT) with atomic database
x-ray emission/absorption, photoionization

Density
Temperature
Emissivity of
K-α, Bremsstrahlung

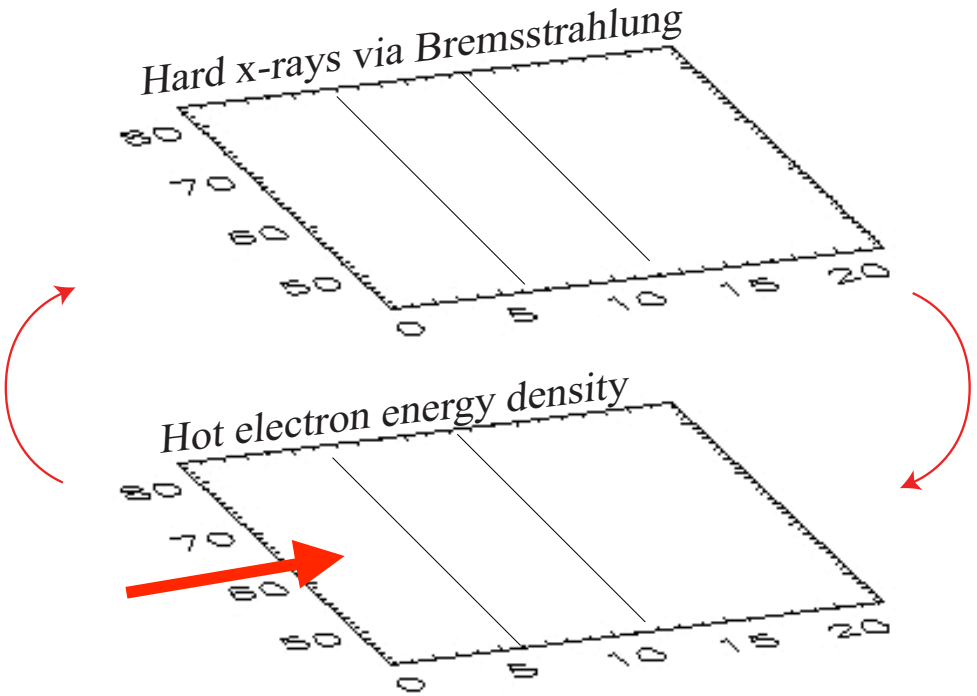

Radiation energy or deposition
Photoelectrons

Copper thin target irradiated 10^{20} W/cm^2 /30fs/5um

Particle-in-Cell code (PICLS) with collision/ionization
laser plasma inetraction, kinetic plasma dynamics

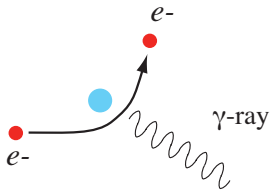

Bremsstrahlung from non-relativistic to relativistic electrons

Koch and Motz formula (Rev. Mod. Phys. 1959)

Photon energy

$$d\sigma_k = \frac{Z^2 r_0^2}{137}\frac{dk}{k}\frac{p}{p_0}\left\{\tfrac{4}{3} - 2E_0E\left(\frac{p^2+p_0^2}{p^2p_0^2}\right) + \frac{\epsilon_0 E}{p_0^3} + \frac{\epsilon E_0}{p^3} - \frac{\epsilon\epsilon_0}{p_0 p} + L\left[\frac{8E_0E}{3p_0p} + \frac{k^2(E_0^2E^2+p_0^2p^2)}{p_0^3p^3} + \frac{k}{2p_0p}\left(\left(\frac{E_0E+p_0^2}{p_0^3}\right)\epsilon_0 - \left(\frac{E_0E+p^2}{p^3}\right)\epsilon + \frac{2kE_0E}{p^2p_0^2}\right)\right]\right\},$$

where

$$L = 2\ln\left[\frac{E_0E+p_0p-1}{k}\right]; \quad \epsilon_0 = \ln\left(\frac{E_0+p_0}{E_0-p_0}\right); \quad \epsilon = \ln\left(\frac{E+p}{E-p}\right).$$

Angular distribution

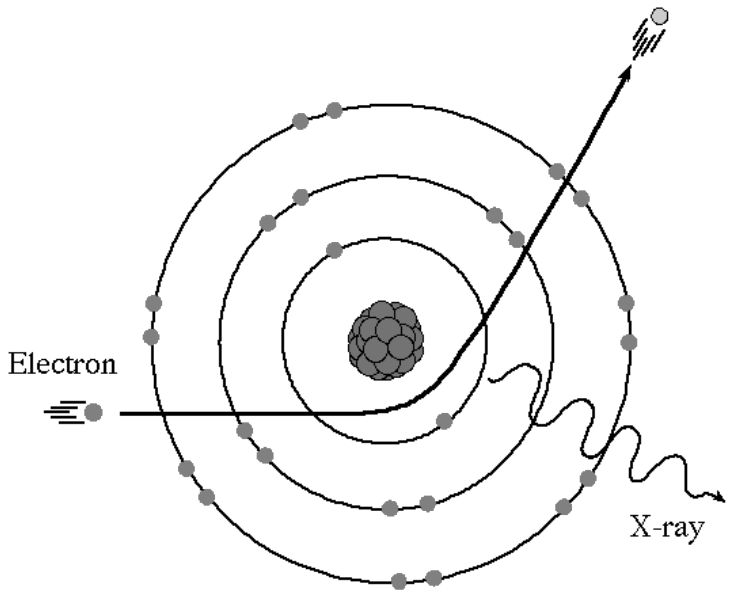

$$\frac{d^2\chi_R}{d\omega d\Omega_\gamma} \simeq \left[\frac{3}{2\pi}\gamma^2\frac{(1+\gamma^4\theta^4)}{(1+\gamma^2\theta^2)^4}\cdot\frac{d\chi_R}{d\omega}\right]$$

Photons are emitted in all angles following he angular distribution for each photon energy.

Electron energy is reduced every time-step to pay all photon energies via bremsstrahlung.

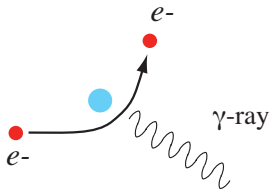

Bremsstrahlung from Relativistic Electrons

J. Jackson, “Classical Electrodynamics”

Photon energy

$$\frac{d\chi_R}{d\omega} \simeq \frac{16}{3}\frac{Z^2e^2}{c}\left(\frac{e^2}{m_ec^2}\right)^2\left(1-\frac{\hbar\omega}{E}+\frac{3\hbar^2\omega^2}{4E^2}\left[\ln\left(\frac{2EE'}{m_ec^2\hbar\omega}\right)-\frac{1}{2}\right]\right)$$

Angular distribution

$$\frac{d^2\chi_R}{d\omega d\Omega_\gamma} \simeq \left[\frac{3}{2\pi}\gamma^2\frac{(1+\gamma^4\theta^4)}{(1+\gamma^2\theta^2)^4}\cdot\frac{d\chi_R}{d\omega}\right]$$

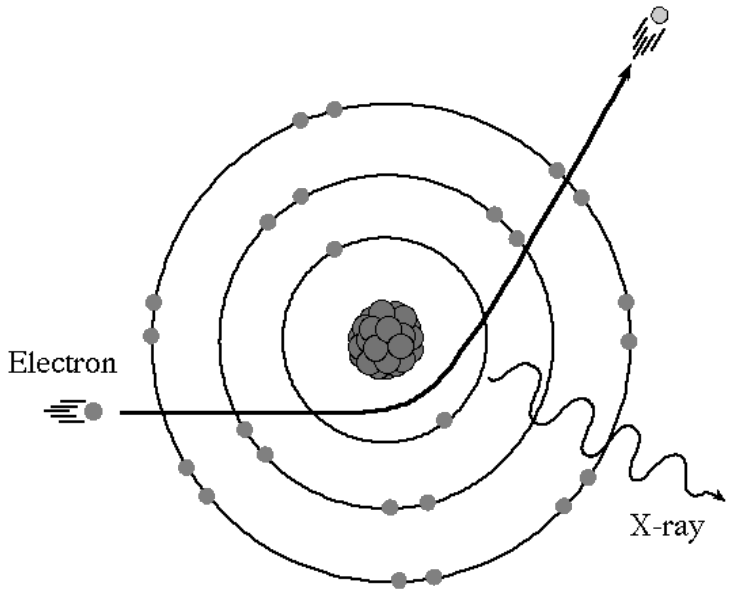

Photons are emitted in all angles following he angular distribution for each photon energy.

Electron energy is reduced every time-step to pay all photon energies via bremsstrahlung.

Bremsstrahlung from non-relativistic electrons is calculated from the emissivity in the precomputed database.
(uniformly emitted)

Comparison between the Koch and Motz formula (Rev. Mod. Phys. 1959) and the Jackson formula for an Aluminum target

The Jackson formula underestimates Bremsstrahlung emission at low electron energies

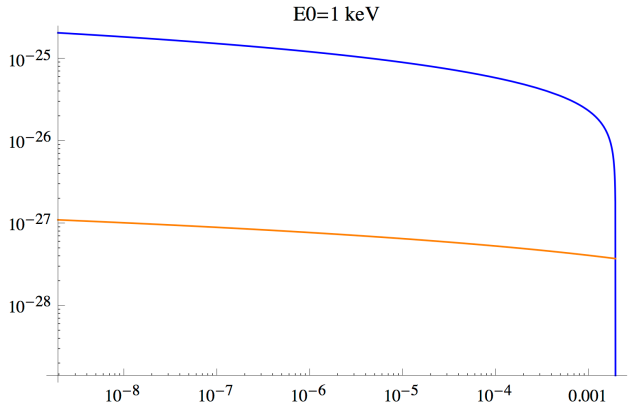

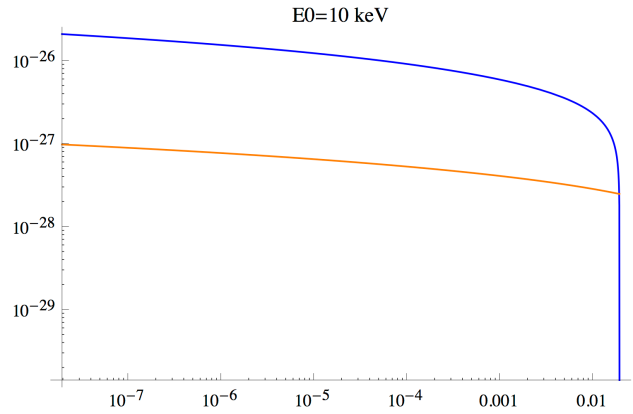

— Koch and Motz

— Jackson

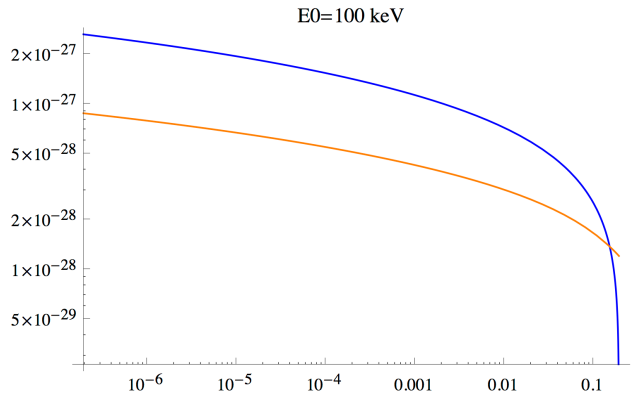

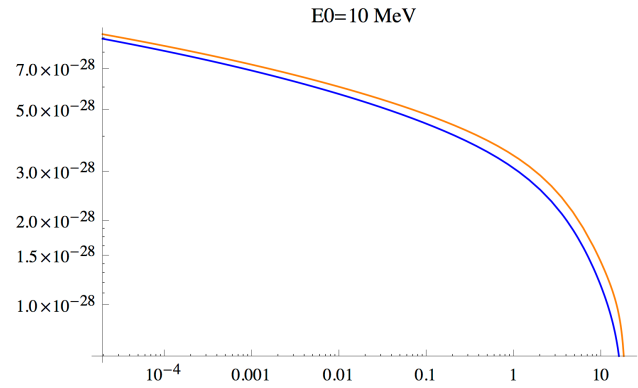

XFEL-matter interaction

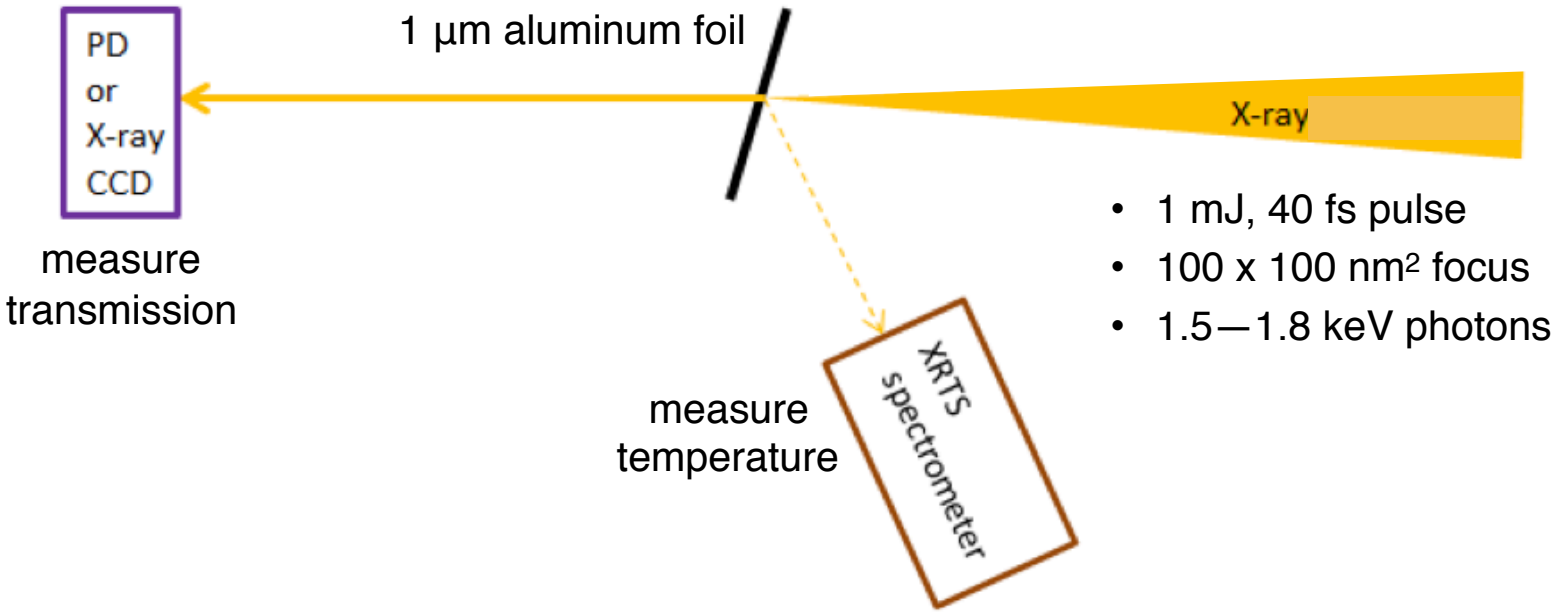

To simulate the XFEL-matter interaction, what we should prepare for?

Model for XFEL-matter interaction: Photoionization is the dominant absorption mechanism for x-rays

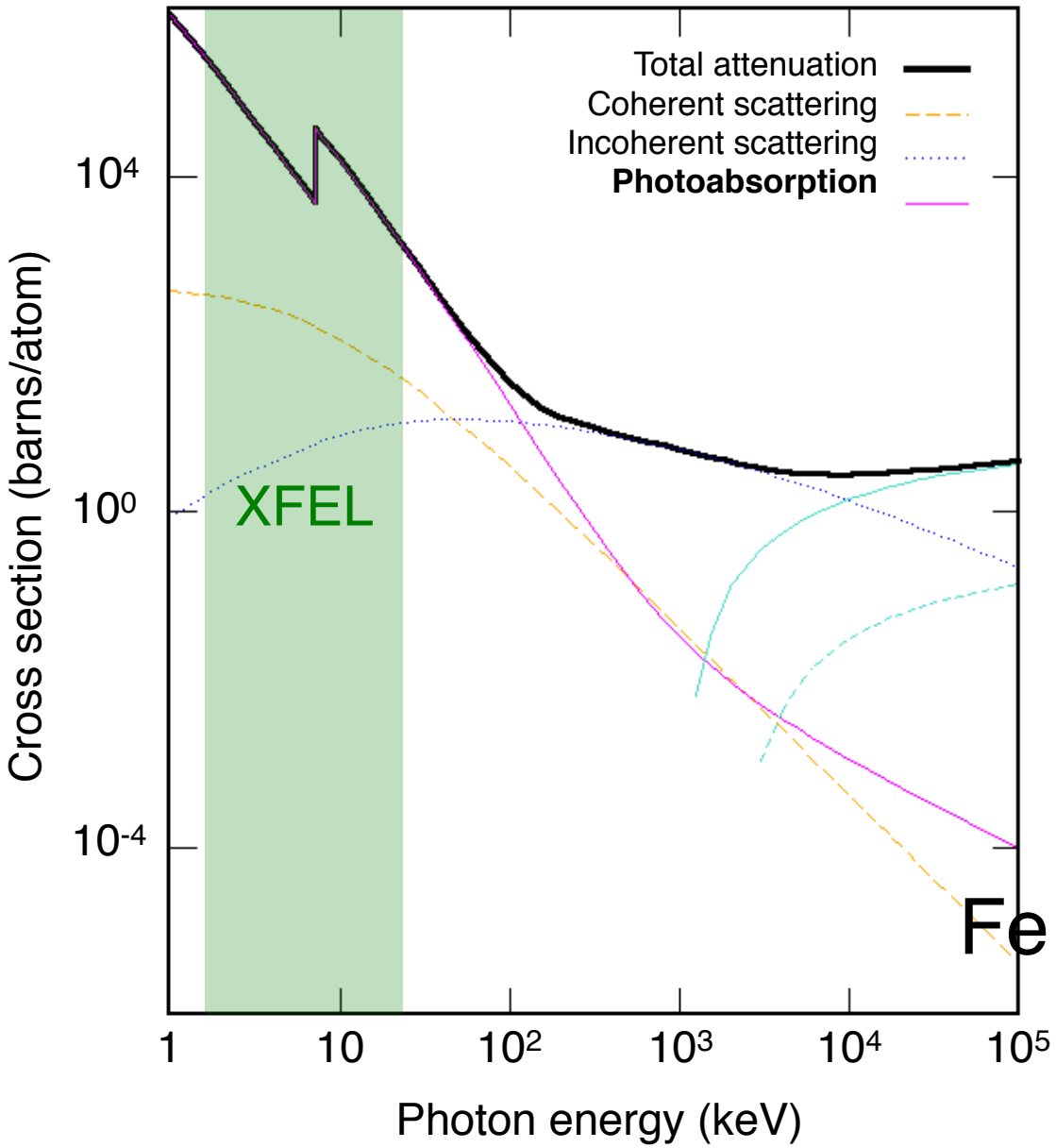

http://www.nist.gov/pml/data/xcom/

Photoionization and Auger ionization

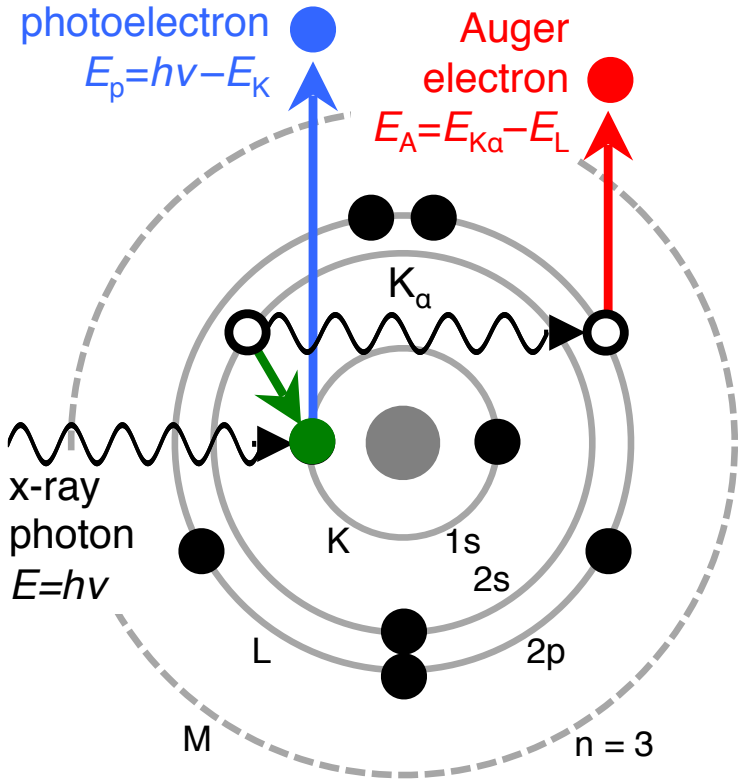

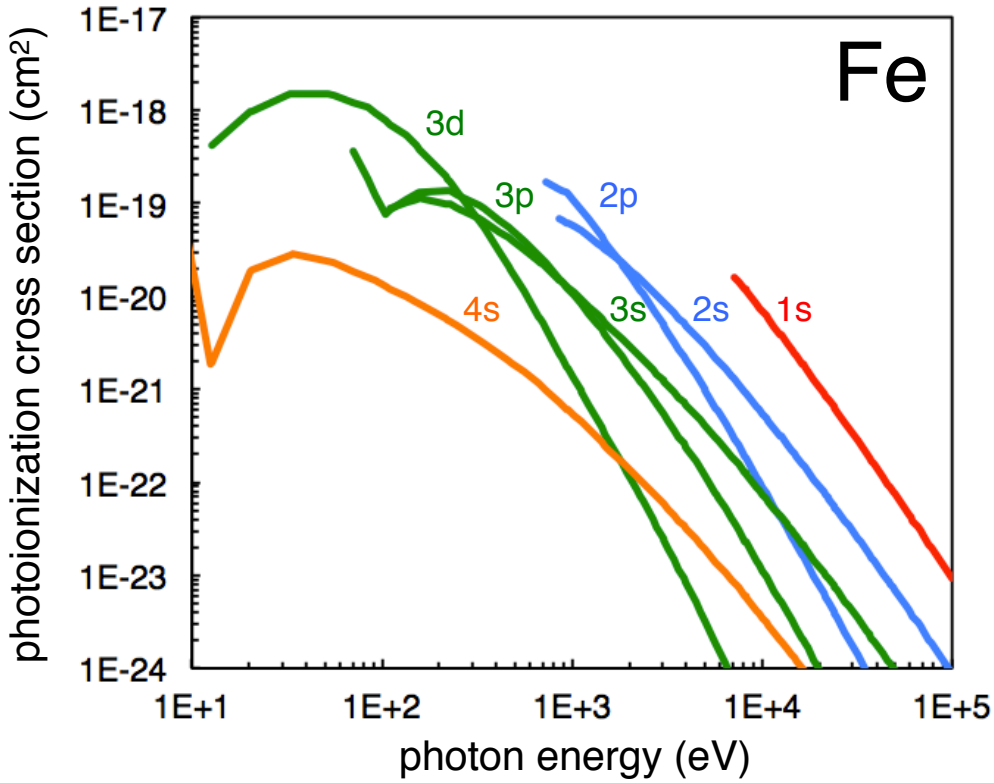

- Neutral-atom suborbital cross sections (right) are precalculated for each element.
- Inner-shell cross sections are constant with ion charge, though edges are blueshifted.
- The dominant relaxation process for low-Z and mid-Z atoms is non-radiative (Auger).
- Only consider KLL Auger ionization is currently modeled.

Ref. LANL Cowan code: http://aphysics2.lanl.gov/tempweb/lanl/

Auger electron energies for the elements

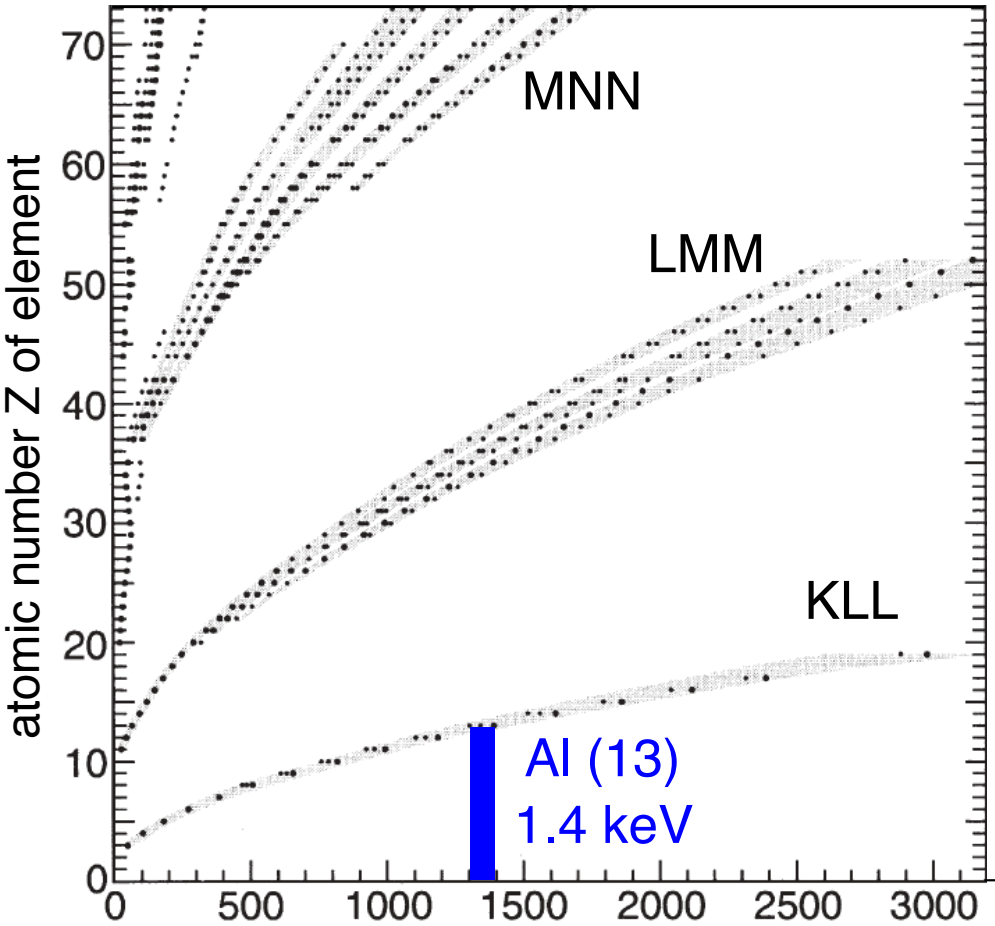

- KLL Auger electron energies increase rapidly with Z.
- LMM Auger electrons have low energies for mid-Z elements, but affect the charge state distribution.

$$E_{KLL} \approx E_K - 2E_L$$

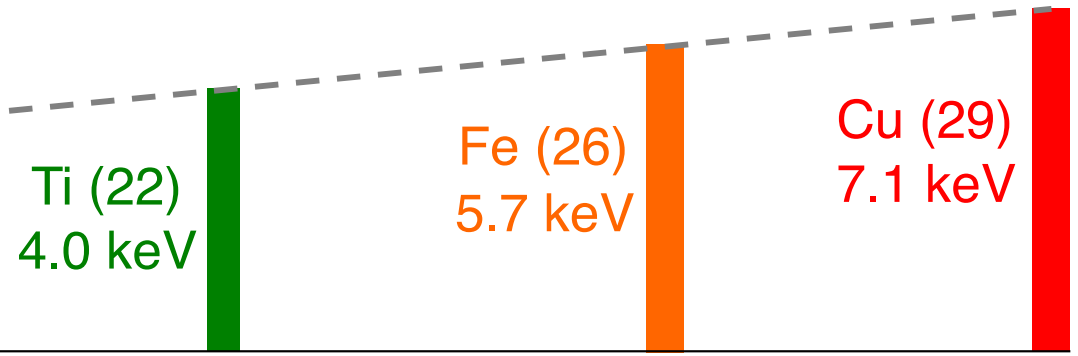

—C. L. Hedberg *et al.*, *Handbook of Auger Electron Spectroscopy*. Physical Electronics Inc. (1995)

Average K-shell vacancy lifetimes

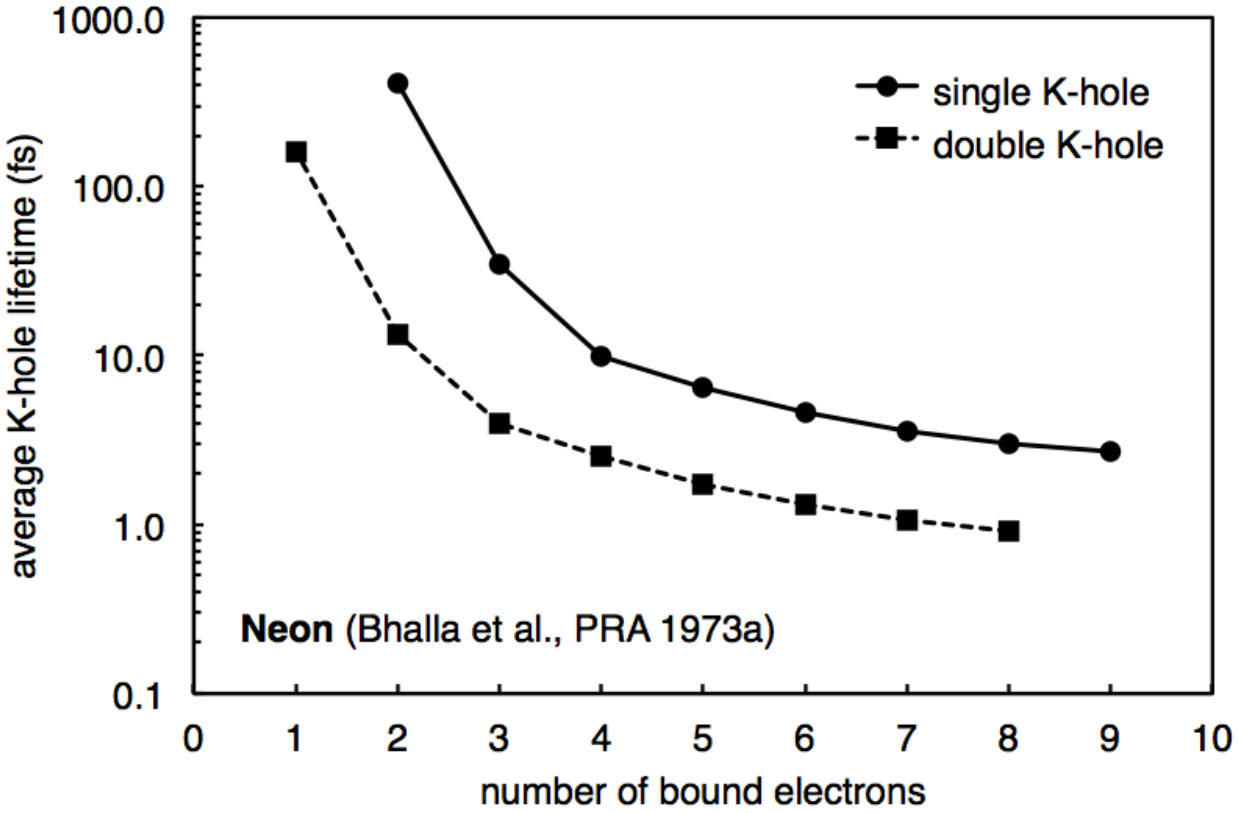

induced transparency

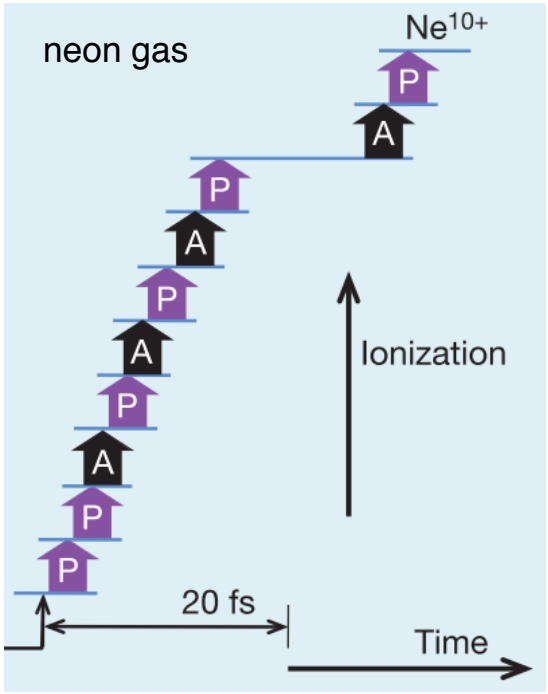

- Simple model uses scaled neon configuration-averaged lifetimes fit to available data.
- K-shell vacancy lifetimes are large for highly ionized and low-Z atoms.
- A “hollow” atom missing both K-shell electrons is mostly transparent to x-rays.

—C. P. Bhalla *et al.*, Phys. Rev. A (1973)

Upshift of orbital energies with charge state

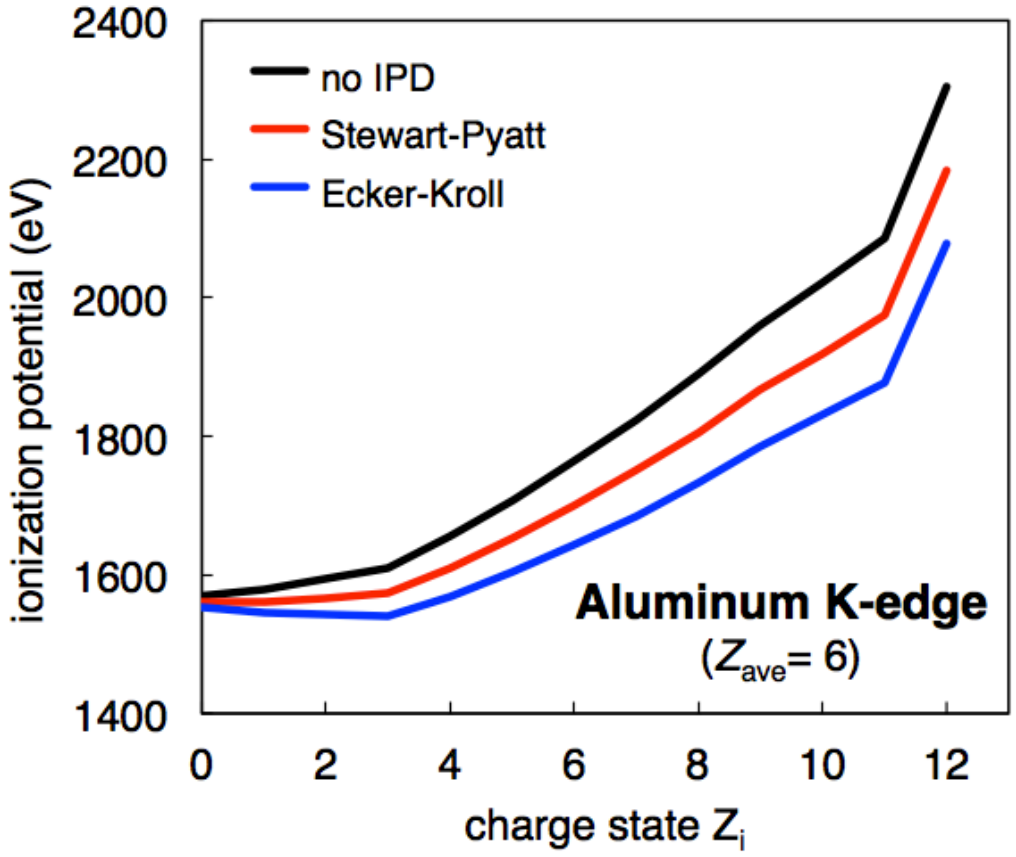

Orbital binding energies, including K-edge, are upshifted by the charge state Z_i.

LCLS experiment for saturable absorption of K-edge

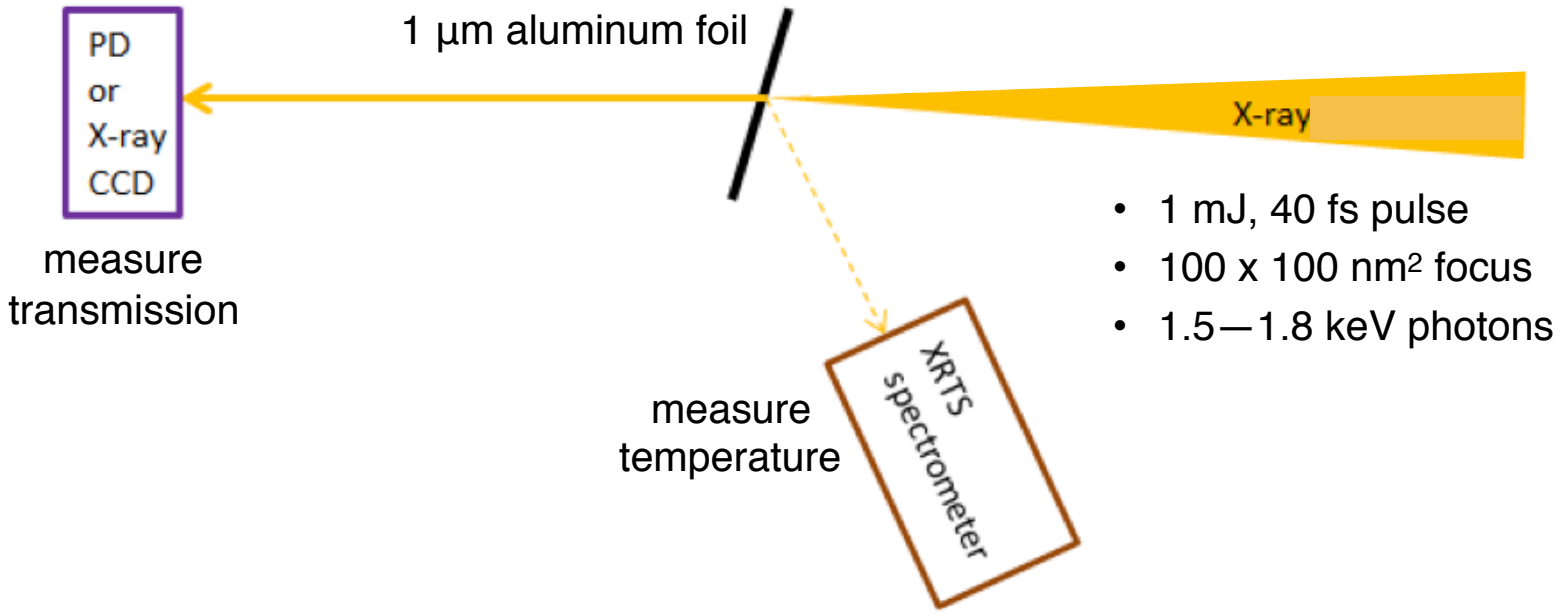

Experimental goals of interest

- Changing the XFEL photon energy in a range of 1500 - 1900 eV, see the transmission.

hν-dependent saturable absorption

- **Decreasing absorption with decreasing *photon energy*.**
- Blueshifted K-edge eventually surpasses X-ray photon energy as ion charge state increases.

D. Rackstraw 2015 (LCLS)

solid aluminum K-shell SA

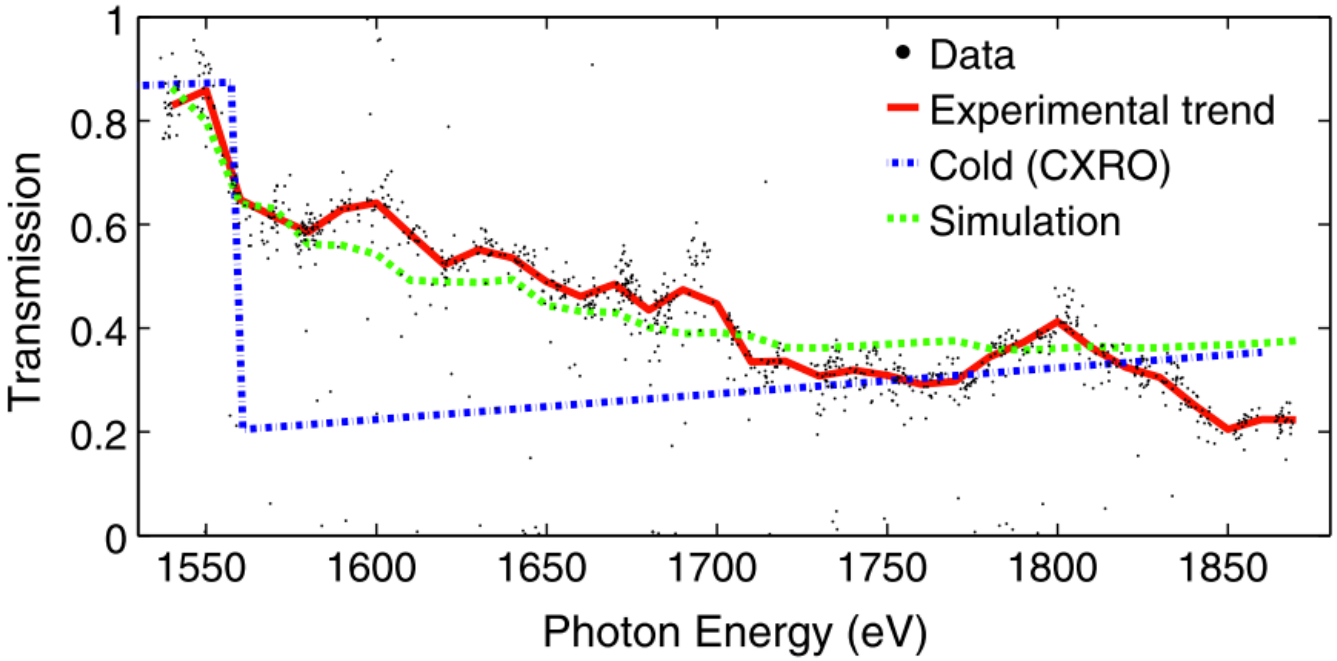

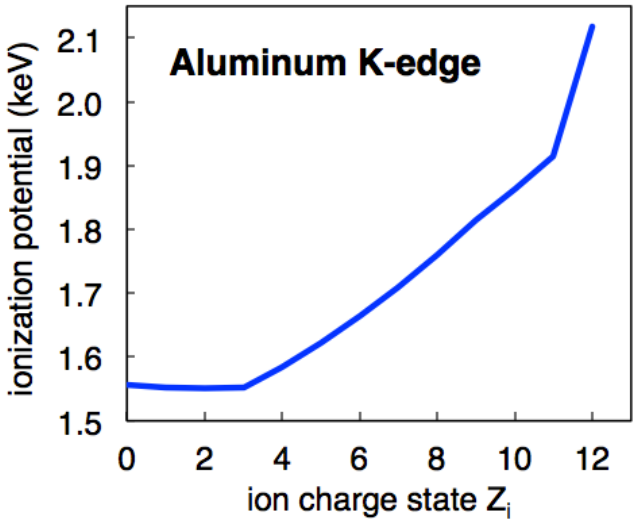

—D. S. Rackstraw *et al.,* Phys. Rev. Lett. (2015)

Simulations of *hv*-dependent SA in aluminum (Rackstraw *et al.*, LCLS, 2015)

Simulation parameters:

1.4 μm solid Al target and 0.6 mJ

50 fs (flat-top) XFEL pulse with 7 μm² super-Gaussian spot (~2e17 W/cm²)

Photon energy varies between 1540—1870 eV.

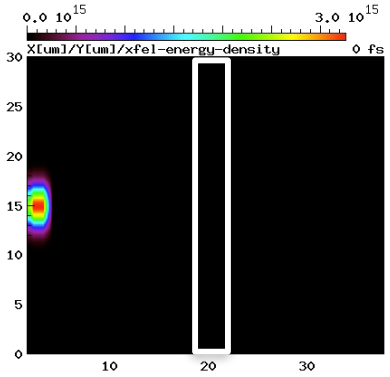

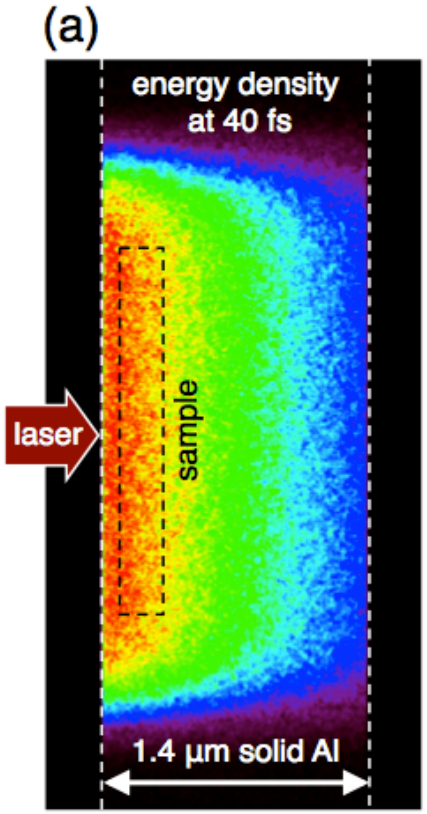

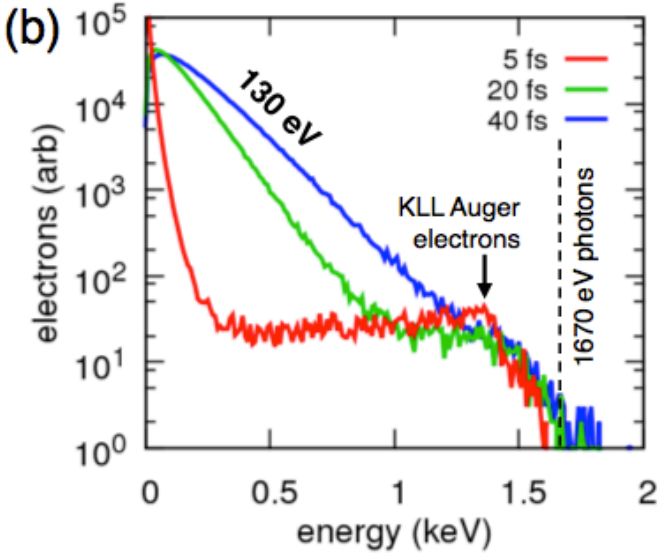

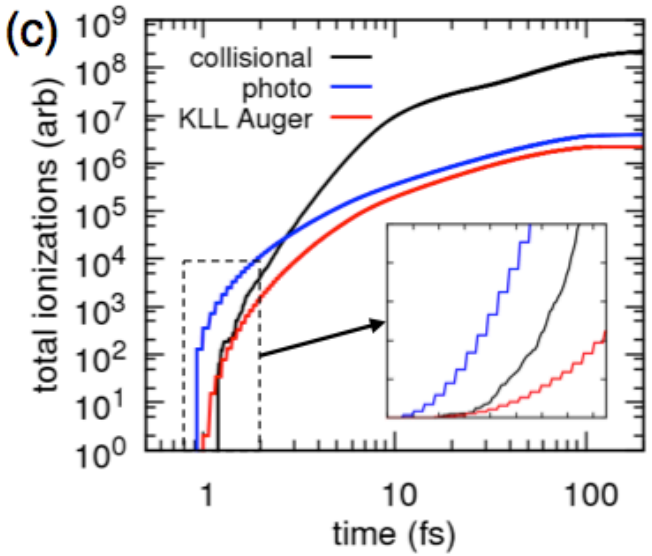

KLL Auger electrons are thermalized via ionization and collisional processes in time scale of 40fs.

Comparing the transmission with experiment with different IPD models

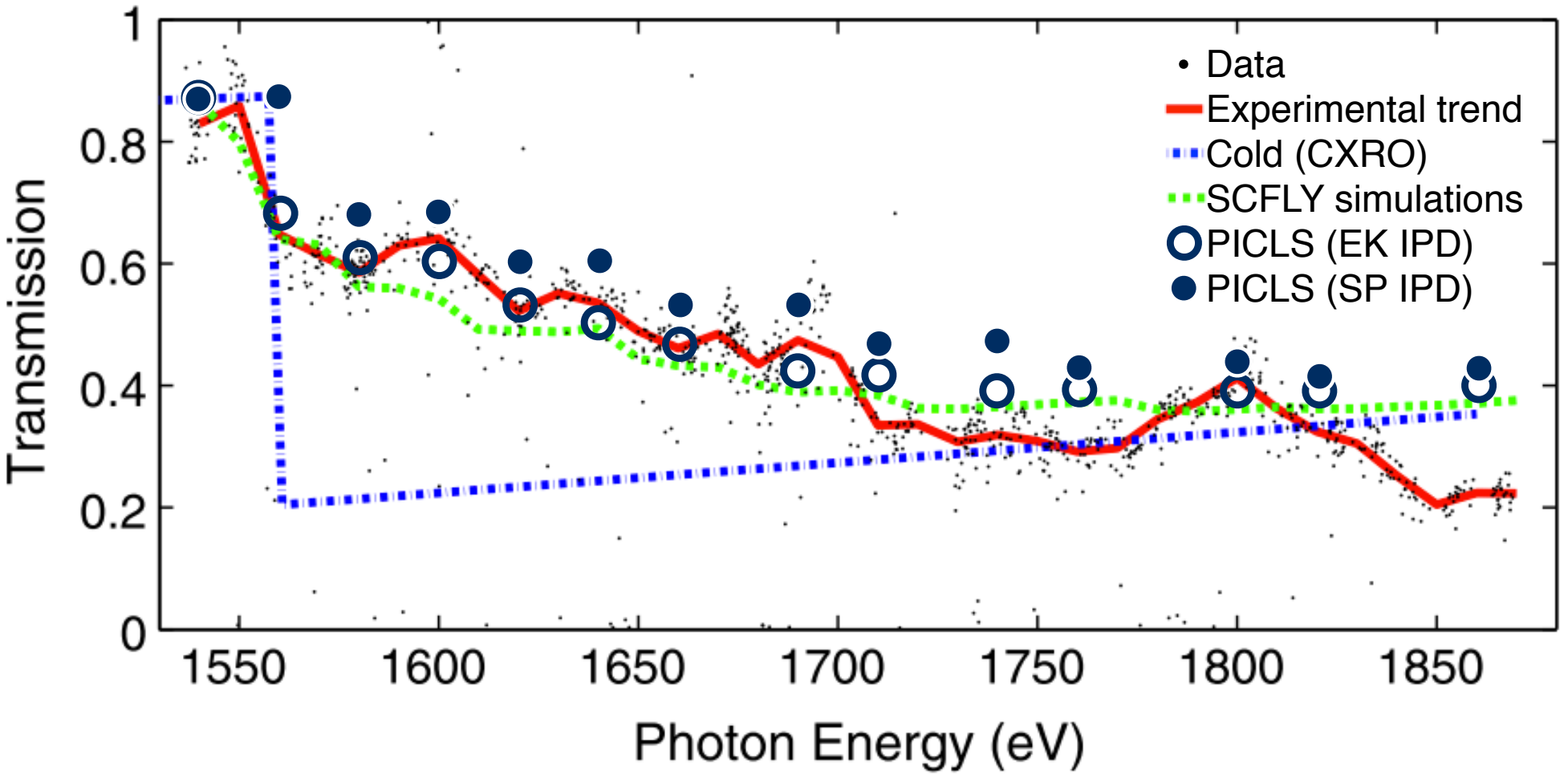

—D. S. Rackstraw *et al.,* Phys. Rev. Lett. (2015)

Summary

- We have developed 2D Particle-in-Cell, PICLS, with Radiation Transport code, that can self-consistently model the laser-plasma formation and development, and the subsequent X-ray radiation emission and transport.
- The photoionization as a single photon model is implemented in the code. This allows us to simulate the XFEL - matter interaction.
- We had performed simulations of XFEL-matter interaction for LCLS experiment, and study the saturable absorption of K-edge. The simulation results are fairly consistent with the experiment.
- Ecker-Kroll model is better for this type of experiment than Stewart-Pyatt model.

This work was supported by DOE/OFES under Contract No. DE-SC0008827 and KAKEN No. 15K21767.

今後のコード開発

- イオン化モデル：イオン化ポテンシャルのダイナミックな更新 (IPD, イオン化度により)。Field Ionizationの超高強度 (>10^{22} W/cm^2)での高精度化。
- ピコ秒超のレーザープラズマ相互作用を安定に計算する境界条件の模索

他にご要望はありますでしょうか？

This work was supported by DOE/OFES under Contract No. DE-SC0008827 and KAKEN No. 15K21767.